Analysis of the October 27, 2025, Sındırgı (Balıkesir) Earthquake together with the recent two events in Western Anatolia

(together with the contributions of Prof. Dr. Erhan Altunel and Prof. Dr. Ali Pınar)

1. Introduction

On October 27, 2025, at 22:48 local time (GMT +3), an earthquake with a magnitude of M_w 6.1 occurred in the vicinity of the Sındırgı district (Balıkesir). The focal mechanism solution provided by AFAD reported the earthquake depth as 6 km and the style-of-faulting as **normal**. A similar focal mechanism solution was also provided by the Kandilli Observatory and Earthquake Research Institute (KOERI) of Boğaziçi University. **The October 27 earthquake**, **which did not produce any surface rupture**, was **manifested as two successive ruptures**, as explained in the following sections in the report. The first rupture (M_w 5.8) occurred on a strike-slip segment by the release of stress that was accumulated after the **August 10** (M_w 6.1) Sındırgı earthquake. **Two seconds after** the first rupture, the second earthquake occurred on a **normal fault** (M_w 6.0). **The M_w 6.0 rupture scenario was considered in the ground motion calculations presented in this report.**

As stated in the following sections, **considering the historical seismic activity of the Western Anatolia Region, potential earthquakes of magnitudes between M_w 6.0 and 6.5 that do not rupture at the surface may occur in the area**. Given the complex seismotectonic structure in the region, **earthquakes of similar magnitudes may trigger each other after a certain time interval as in case of 10 August and October 27 events**.

2. Ground Motion Distribution

The October 27 Sındırgı earthquake was felt within a radius of approximately 300 km, encompassing major cities such as Istanbul, Izmir, Çanakkale, and Bursa. Figure 1 shows the intensity maps generated for this earthquake using AFAD's strong ground-motion station recordings as well as the T-Rupt ground-motion model.

Figure 1 (top panel) presents a map showing the spatial variation of horizontal peak ground velocity (PGV) across geographic locations. The horizontal component definition of PGV is geometric mean, and the map is plotted for median PGV. This map indicates that in the vicinity of epicenter, the ground velocity reaches to 20 cm/s, while in the city center of Balıkesir, PGV values range between 0.9 cm/s and 2.0 cm/s. The bottom panel of the same figure shows the corresponding macroseismic intensity map, **MMI (**derived from the given PGV distribution). The MMI within the epicentral region ranges between **VII** and **VIII**. Such intensities are indicators of "*light and/or minor damage for well-designed buildings and severe damage or even collapse for poorly designed structures.*" The macroseismic intensity ranges between **IV** and **V in the center of Balıkesir city**. These intensity levels are representatives of "*vibratory motion felt by many people, and toppling/breaking of household items.*" In Istanbul and surrounding areas, the macroseismic intensity was determined as MMI III, which reflects a level where the earthquake "*may be felt only by a few people.*"

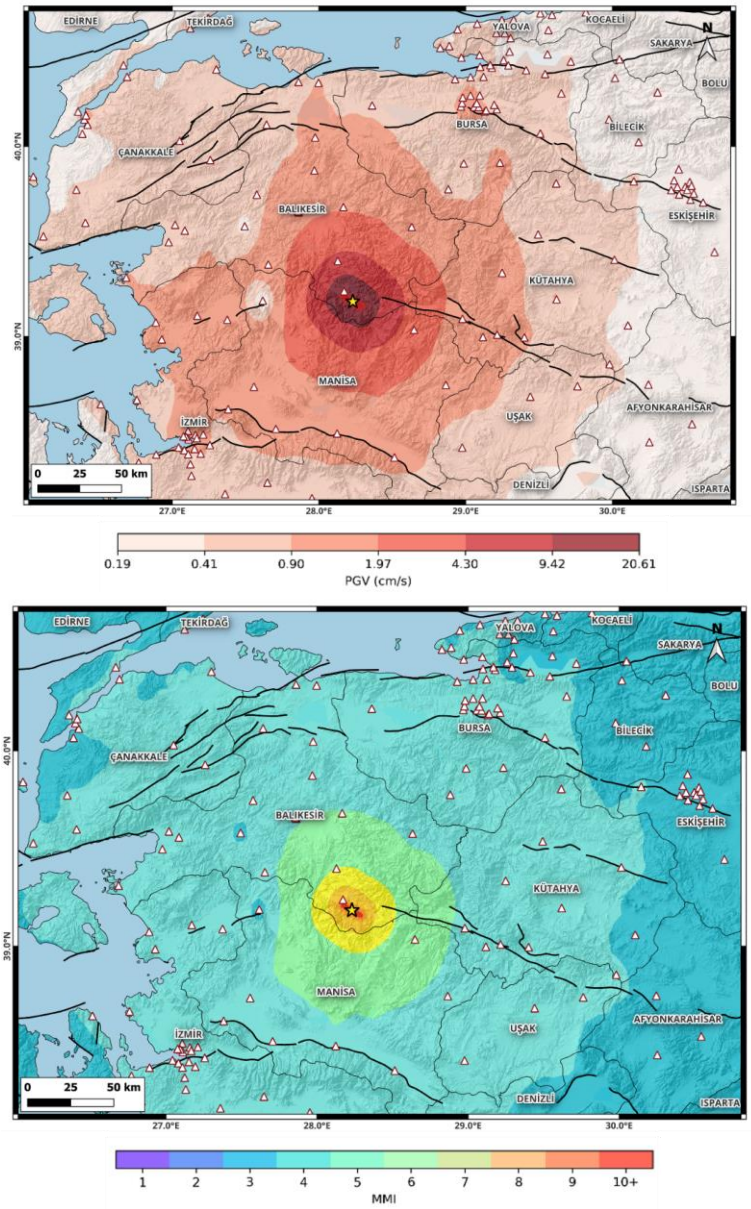

Figure 1*. Shakemaps. Top panel: geographic distribution of median PGV. Bottom panel: geographic distribution of macroseismic intensity. The white triangles indicate the locations of AFAD stations that recorded strong ground-motion data from the 27 October Sındırgı earthquake. The data were used in the calculation of the PGV and macroseismic intensity values given in the maps.*

Figure 2 compares the horizontal geometric mean PGV values recorded by AFAD stations with those predicted by the T-Rupt ground motion model. The comparisons show that the T-Rupt model captures the random variability of ground motions well within ±σ band. Although this comparison is specific to this earthquake, it can advocate that the T-Rupt ground-motion model is a consistent one for estimating the vibratory ground motions in Türkiye.

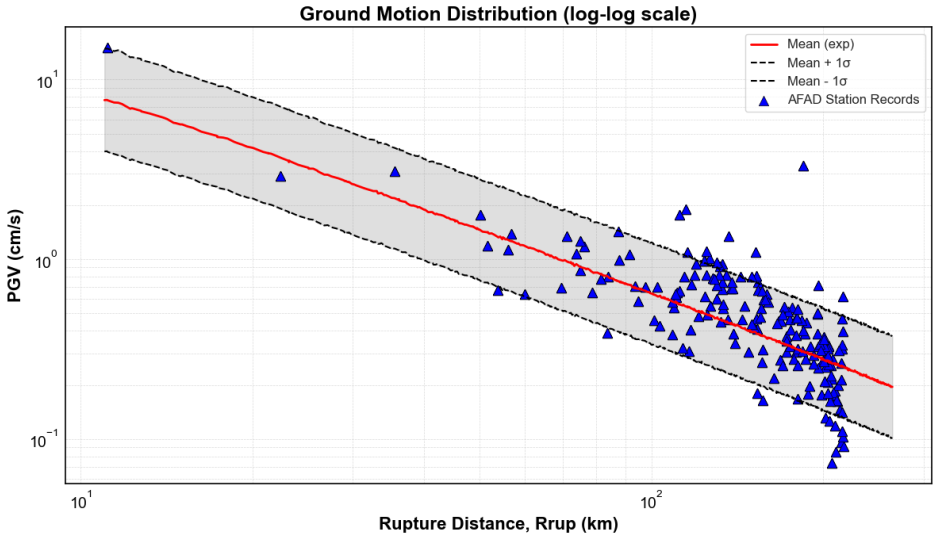

***Figure 2**. Comparisons between the horizontal geometric mean PGV values calculated from the acceleration records of AFAD and their counterparts predicted by the T-Rupt ground-motion model for the 27 October Sındırgı earthquake. All PGV values from AFAD were adjusted to reference site conditions (V_{S30} = 760 m/s). Similarly, the T-Rupt ground motion model predictions represent reference site conditions.*

3. General Tectonic Framework of Western Anatolia

Türkiye is located between the Eurasian and African-Arabian plates. The two active tectonic features in the Anatolian peninsula were formed due to the tectonic motion of these blocks. These active tectonic features are the right-lateral North Anatolian Fault Zone (NAFZ) and the left-lateral East Anatolian Fault Zone (EAFZ). The tectonic regions known as the Western Anatolia "Extensional" Region and the Central Anatolia "Basin" Region are moving westward along the NAFZ and EAFZ (Figure 3).

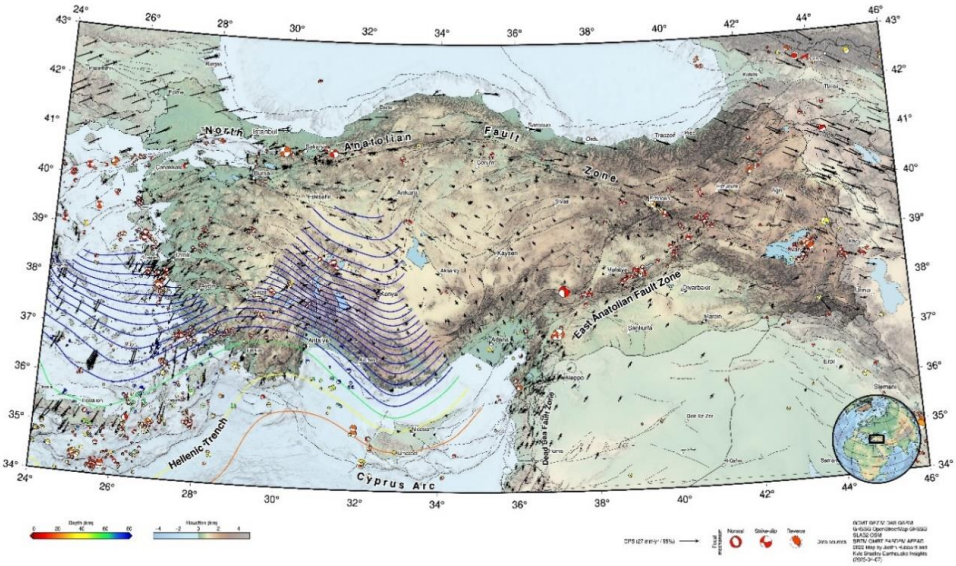

Figure 3. Seismotectonic map of Türkiye. The wavy curves (contour lines) indicate the depth variations of subduction surfaces extending into the crust, resulting from the subduction of the Mediterranean seafloor beneath the Anatolian Peninsula and the Aegean Sea. The black arrows show the direction and velocity of crustal movement based on GPS data. These GPS measurements demonstrate that the Western Anatolia "Extensional" Region and the Central Anatolia "Basin" Region are moving westward.

The westward movement of the Anatolian Block causes the Western Anatolia Extensional Region to undergo extension approximately in the **north-south** direction. As a result of this deformation, the region features east–west oriented grabens and elevated blocks (horsts), bounded by active **normal faults** (Figure 4).

The main grabens of the Western Anatolia Extensional Region, from south to north, are the Gökova, Büyük Menderes, Gediz, and Bakırçay (Bergama) grabens (Figure 4). The normal faults that bound these grabens are the region's most significant earthquake sources. The horst-graben morphology becomes less prominent toward the north, where smaller-scale grabens are observed, such as the Simav graben.

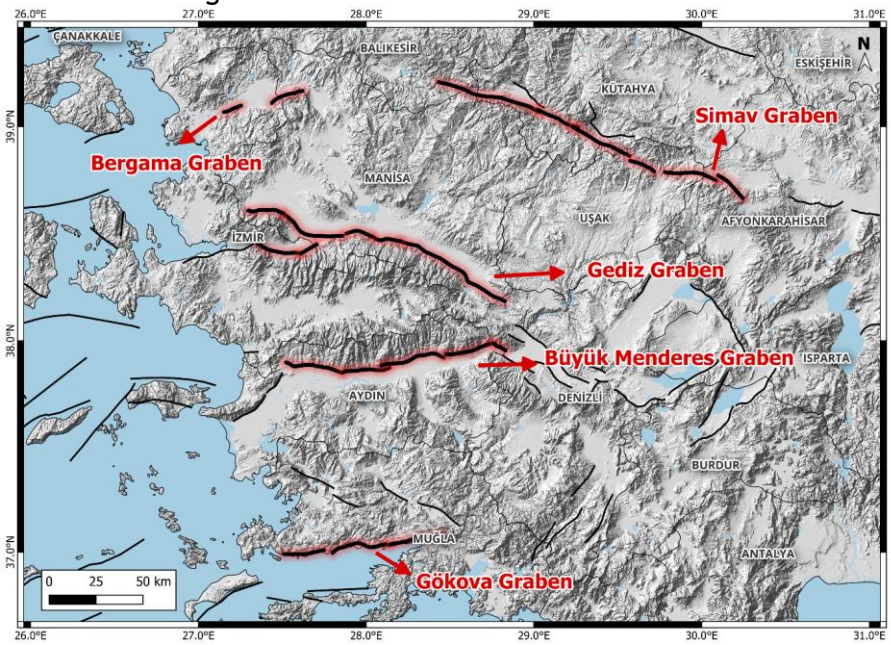

Figure 4. Active faults and major morphological structures in Western Anatolia.

4. The Sındırgı and Simav Earthquakes

Figure 5 shows the epicenters of the August 10 Sındırgı (M_w 6.1), September 28 Simav (M_w 5.5), and October 27 Sındırgı, earthquakes that occurred in the Western Anatolia "Extensional" Region. The **September 28 Simav earthquake** occured on a **normal fault** bounding the northern edge of the Simav Graben. The **August 10 Sındırgı earthquake** occurred on a NW–SE trending, **north-dipping normal fault**, as indicated by its focal mechanism (Figure 5). Although the NW-SE trending fault suggested for the August 10 Sındırgı earthquake aligns with the morphological linearity marking the southern boundary of the basin to west of Sındırgı, the field surveys along this lineament have not revealed any footprints of surface rupture advocating the presence of an active fault.

The focal mechanism solution of the **October 27 Sındırgı earthquake** also indicates that the event occurred on a NW–SE trending fault (Figure 5). However, the detailed analysis of seismic records suggests that the earthquake began on a strike-slip fault (M_w 5.8) and, two seconds later, triggered the rupturing of a **normal fault** (M_w 6.0) located southeast of the August 10 earthquake (Figure 6). The NE–SW trending strike-slip fault observed between the two normal faults (those ruptured in the August 10 and October 27 events) can be interpreted either as a transform fault linking the two normal faults, or as a fault acting as a barrier between them.

The epicenter of the October 27 earthquake suggests a **south-dipping normal fault mechanism**. Although there are no footprints of surface faulting for this earthquake (Figure 5), the focal mechanism solution agrees well with a NW–SE trending morphological lineament located approximately 5 km southeast of Sındırgı, near the village of Ilıca. **Therefore, the October 27 earthquake is considered to have occurred on a NW-SE trending, southwest-dipping fault near Ilıca village.**

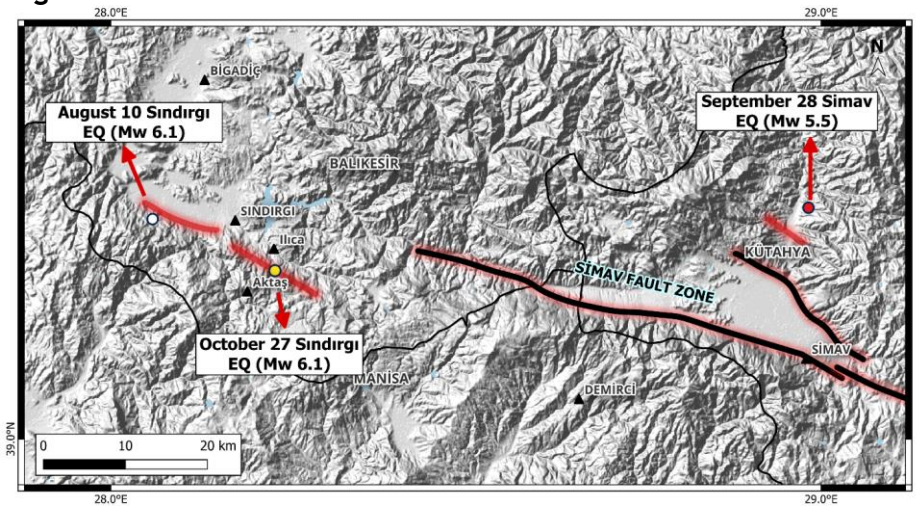

***Figure 5**. Epicenters of the August 10 Sındırgı, September 28 Simav, and October 27 Sındırgı earthquakes along with the surface projections (red lineaments) of their rupture models (based on their focal mechanism solutions).*

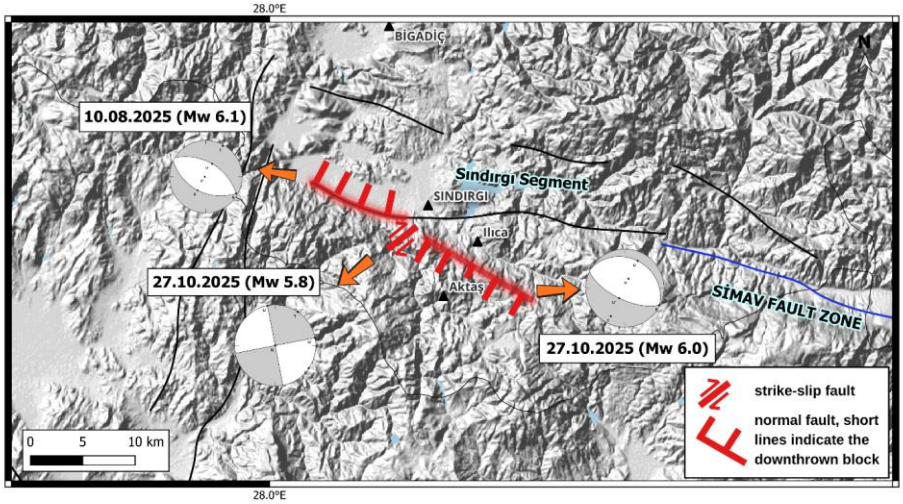

***Figure 6**. Focal mechanism solutions for the August 10 and October 27 Sındırgı earthquakes.*

5. Assessment of the Sındırgı and Simav Earthquakes

Aftershocks that occur on active normal faults typically concentrate on the "hanging wall" block, which moves downward during the mainshock. **However, this is not the case for the three earthquakes discussed in this report, all of which exhibit normal fault rupture characteristics**. When the distributions of their aftershocks are examined, one infers that the aftershocks are spread over a wide area and as noted above they extend well beyond the boundaries of the hanging wall block (Figure 7).

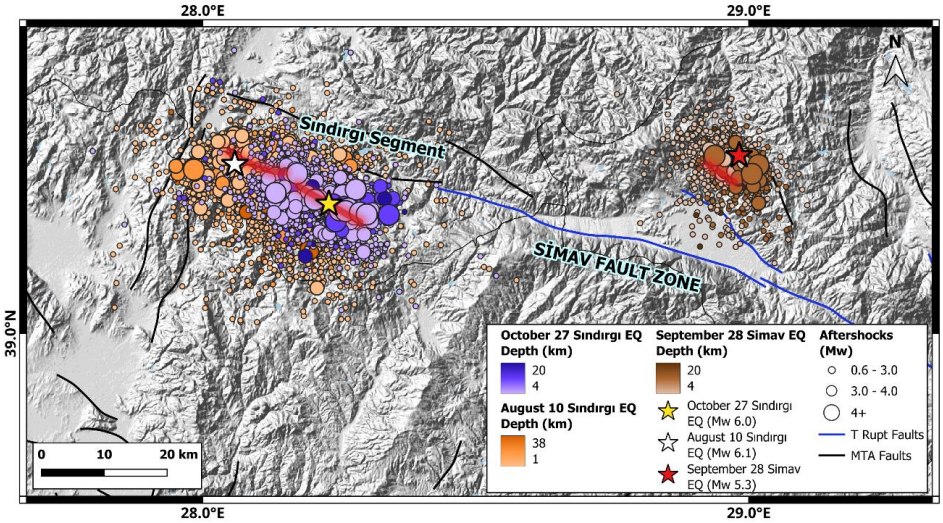

***Figure 7**. Aftershock distributions of the August 10 (white star), September 28 (red star), and October 27 (yellow star) earthquakes. The red lines represent the surface projections of their ruptures modeled based on the focal mechanism solutions.*

Among these three earthquakes, the August 10 and October 27 events that occurred near the Sındırgı town do not exhibit clear geological or morphological traces at the surface. This observation suggests the existence of several faults capable of generating earthquakes of magnitudes between $6 \leq M_w \leq 6.5$ without showing a rupture trace at the surface. As a supporting argument to this observation, Figure 8 shows a significant number of historical earthquakes of $6 \leq M_w \leq 6.5$ from the region that did not rupture at the surface.

Despite the absence of clear surface traces, which could be considered as the indicator of active faults, the intense seismic activity around Sındırgı might lead to the interpretations suggesting volcanic activity originated seismicity. However, such an interpretation is unrealistic as the nearest volcanic vent (from late Quarternary –12,000 years ago-) that can be associated with volcanic activity is located near Kula, 70 km southeast of Sındırgı. ın other words if magma flow due to volcanic activity ever existed, it would have followed its previous path to emerge at the surface that is 70 km southeast of Sındırgı.

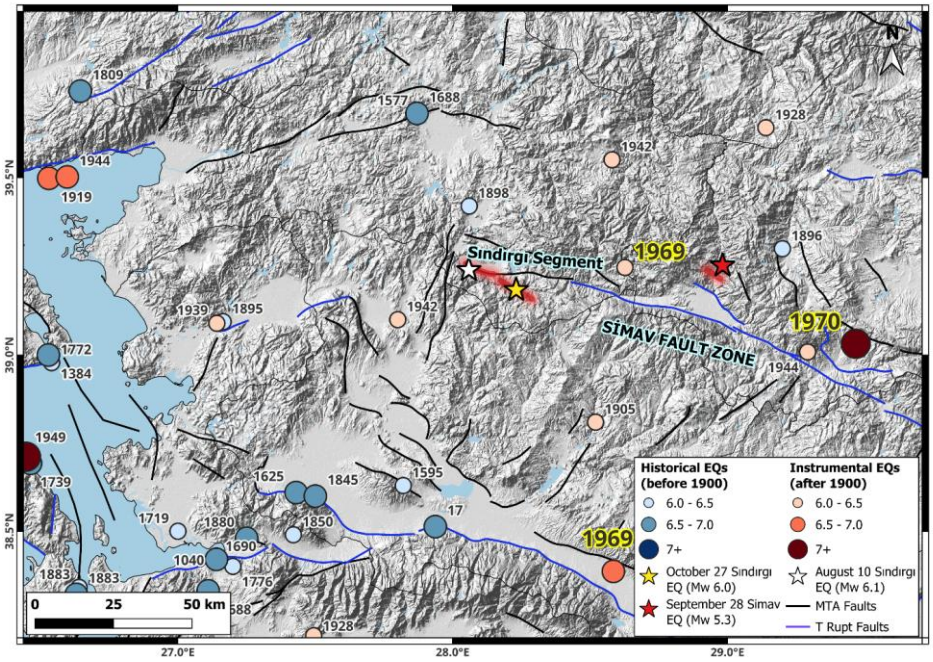

***Figure 8**. Geographical distribution of historical earthquakes with magnitudes of M_w 6.0 and above in the Western Anatolia Extensional Region (T Rupt historical earthquake catalog).*

6. Final Remarks

There is no geological or morphological evidence around Sındırgı advocating a tectonic structure (i.e., active faults) that leaves its footprints on the surface morphology, which is the case in the Gökova, Büyük Menderes, Gediz, and Bergama grabens. Nevertheless, the region continues to experience moderate-magnitude earthquakes (M6.0–6.5) during both historical and instrumental periods (Figure 8).

There is currently no tectonic structure (i.e., faults) in the region that has developed in response to the prevailing north–south oriented extensional stress. The wide spatial distribution of aftershocks further supports this observation.

Within the geographical boundaries of Türkiye, the crust has undergone intense deformation due to significant orogenic (i.e., formation of mountain chains) processes. Each tectonic phase during these orogenies formed its own deformation patterns, such as faults, folds, and fractures. The deformation structures from earlier tectonic periods, known as paleotectonic structures, now serve as zones of weakness within the crust. Under the current tectonic regime, the north-south oriented extensional stress accumulates deformation energy, which is released through these weak zones. Therefore, the earthquakes occurring in the Sındırgı region are local events resulting from the release of stress accumulated along paleotectonic faults under the present-day tectonic regime.

Based on these evaluations, continued seismic activity in the region is considered to be normal; however, the likelihood of a surface-rupturing earthquake of significant magnitude is estimated to be low.